Int. J. Solids Structures, 1972, Vol. 8, pp. 193 to 214. Pergamon Press. Printed in Great Britain

THE MEASUREMENT OF RESIDUAL STRESSES BY THE USE OF PHOTOELASTIC GAUGES

G. J. MATTHEWS and C. J. HOOKE

Department of Mechanical Engineering, University of Birmingham, Birmingham, England

Abstract—One method of measuring residual stresses in metals is to bond an annular photoelastic disc to the surface of the metal and drill a central hole through the gauge into the underlying material. If the gauge is then viewed in polarized light a fringe pattern is observed. The purpose of this paper is to obtain a simple and accurate relationship between the fringe orders measured and the residual stresses present. Part I deals with the calculation of the displacements in the metal. In Part II the resulting stress situation in the gauge is determined. Calibration factors are then presented for a wide range of gauge geometries.

NOTATION

a	hole radius
b	gauge outside radius
f	fringe stress coefficient for gauge material
r	radius
t	gauge or metal thickness
u	radial displacement
v	hoop displacement
w	axial displacement
B	b/a
N	fringe order
R	r/a
S_1S_2	principal residual stresses
T	t/a
U	u/a
V	v/a
W	w/a
Z	z/a
K, β	constants
τ	stress (using tensor notation)
μ	shear modulus
σ	Poisson's ratio
Subscripts	
g	gauge
b	metal

I. THE DISPLACEMENTS AND STRESSES AROUND HOLES IN PLATES OF ARBITRARY THICKNESS

INTRODUCTION

THE "hole drilling" technique is used for the measurement of either residual or live stresses in an elastic material. The application of this technique involves drilling a small hole to

a limited depth in a stressed material and relating the resulting change in the displacements or strains in the region of the hole to the magnitude and directions of the principal stresses in this region. Nisidi [1] and Nisidi and Takabayashi [2] have developed a method suitable for the practical application of this technique.

In their method, an annular photoelastic disc is bonded to the surface of the metal and a central hole is drilled through the gauge into the underlying metal. If the gauge is then viewed in polarized light a fringe pattern is observed. From the symmetry of this pattern the directions of the principal stresses are readily obtained. Their magnitudes, however, are greatly underestimated if they are calculated using "plane strain" theory unless the gauges used are thin. This error is attributed to "shear lag" i.e. although the strains at the surface of the metal are transmitted faithfully to the base of the gauge they progressively diminish through its thickness and consequently the fringe orders produced are lower than those predicted by simple theory.

The purpose of this paper is to describe a method whereby the effects of shear lag may be accurately predicted and to obtain a simple relationship between the fringe orders measured and the residual stresses present in the metal. Such an analysis may be conveniently considered as two individual problems. The first problem is to determine the change in the displacements at the surface of the metal upon drilling the hole. In solving this problem the stress concentration effect of holes in plates of arbitrary thickness may also be examined. Then, having obtained the displacements at the metal surface, the second problem is to determine the fringe pattern produced in the gauge.

To make the problem of determining the metal displacements more tractable the following assumptions are made:

1. The metal is an elastic, homogeneous, isotropic material.
2. The diameter of the drilled hole is small compared to the overall dimensions of the metal.
3. The modulus of elasticity of the photoelastic material is small compared to that of the metal and hence the reinforcing effect of the gauge on the underlying metal may be ignored.
4. The principal stresses in the region of the point at which their values are to be determined are uniform.

The problem then reduces to a three dimensional boundary value problem involving the determination of the displacements of a cylindrical body whose terminal boundaries are free from loads and whose lateral boundaries have prescribed loads acting upon them. Furthermore, the principal stresses in the region of the hole may be regarded as a linear combination of two basic stress systems. The first is one in which the principal stresses are of the same sign and equal in magnitude and the second is one in which the principal stresses are equal in magnitude but opposite in sign. Having obtained the displacements in the metal for each of these two systems, the displacements for any other stress system may be found by superposition.

CALCULATION OF THE STRESSES AND DISPLACEMENTS

(a) *Equal principal stresses*

The "plane stress" solution for the first system is:

$$2\mu u = \frac{1-\sigma}{1+\sigma} r + \frac{a^2}{r}$$

$$2\mu v = 0$$

$$2\mu w = -\frac{2\sigma}{1+\sigma}z$$

$$\tau_{rr} = 1-\frac{a^2}{r^2}$$

$$\tau_{\theta\theta} = 0{\cdot}1+\frac{a^2}{r^2}$$

$$\tau_{zz} = \tau_{rz} = \tau_{\theta z} = \tau_{r\theta} = 0.$$

This solution satisfies the prescribed boundary conditions of this system and is an admissible solution to the three dimensional problem.

(b) *Equal but opposite principal stresses*

The "plane" solution to the second system satisfies the lateral boundary conditions but gives an erroneous axial stress on the terminal boundary. The failure of this elementary solution to satisfy the boundary conditions of the second stress system necessitates the consideration of existing approximate solutions to the problem [3–7]. It is apparent that the prime purpose of these approximate solutions has been to determine the stress concentration effect of holes in plates of arbitrary thickness. Although these are predicted to an accuracy within the realms of physical significance there are significant discrepancies in the displacement fields established by these techniques. Furthermore, it is difficult to establish a degree of accuracy for any one of these solutions except for that for an infinitely thick plate which is presented by Youngdahl and Sternberg [7].

In order to obtain an accurate analysis of the "shear lag" effect it was considered necessary to obtain the displacement field in the metal precisely and it was therefore decided to solve this problem using the point matching technique. This technique superimposes a number of basic solutions to the elasticity equations so as to approximately satisfy the prescribed boundary conditions at a number of points on the surface of the body. The use of the point matching technique is described in Ref. [8] and the more recent applications of the technique are given in Refs. [9–13].

THEORY

Of immediate interest in the solution of the shear lag problem is the change in the displacement field at the surface of the metal upon drilling a hole in the pre-stressed material. However, from a general engineering aspect it is the total change in the displacement field from the unstressed state that is of major interest as this determines the stress concentration effect of the hole. The difference between these two displacement fields is merely the displacement field produced by loading the metal without the hole present and a well-known solution exists for this problem. It is therefore irrelevant which of the displacement fields is determined. For comparison purposes it is convenient to determine the total change in the displacement field from the unstressed state as this has been the purpose of previous approximate solutions. This will also enable the stress concentration effect of holes in plates of arbitrary thickness to be studied.

The boundary conditions to be satisfied in determining this displacement field are: at $R = \infty$

$$\tau_{RR} = \cos 2\theta \qquad \tau_{R\theta} = -\sin 2\theta \qquad \tau_{RZ} = 0$$

at $R = 1$

$$\tau_{RR} = \tau_{R\theta} = \tau_{RZ} = 0$$

and at $Z = \pm T/2$

$$\tau_{ZZ} = \tau_{\theta Z} = \tau_{RZ} = 0. \tag{1}$$

To satisfy these boundary conditions using the point matching technique it is necessary to determine initially a number of basic solutions to the elasticity equations. Each of these solutions will correspond to a different set of conditions on both the terminal and lateral boundaries of the plate. The boundary conditions given by equation (1) are then approximately satisfied by superpositioning these basic solutions, so as to minimize the sum of the squares of the errors in the boundary conditions at a number of points on the surface (see Appendix 1). It is advantageous in this technique to choose solutions that individually approximate to the actual stress distribution in the body so as to reduce the number of basic solutions needed to obtain a specified accuracy.

From considerations of the symmetry of the plate it is reasoned that the radial and circumferential displacements are symmetrical and the axial displacements are skew symmetrical about the mid-section of the plate. The basic solutions which are to be superpositioned to yield the final approximate result must also have this symmetry and this leads to a choice of basic displacement functions of:

$$\begin{aligned} U &= \bar{u} \cos KZ \cos 2\theta \\ V &= \bar{v} \cos KZ \sin 2\theta \\ W &= \bar{w} \sin KZ \cos 2\theta \end{aligned} \tag{2}$$

where the line $Z = 0$ corresponds to the mid-section of the plate, and $\bar{u}, \bar{v}, \bar{w}$, are determined by initially substituting equations (2) into the stress–displacement equations of elasticity to obtain the following stresses:

$$\frac{\tau_{RR}}{2\mu_b \cos 2\theta} = \left(\frac{d\bar{u}}{dR} + \beta\right) \cos KZ = \tau_{R\bar{R}} \cos KZ \tag{3}$$

$$\frac{\tau_{\theta\theta}}{2\mu_b \sin 2\theta} = \left(\frac{2\bar{v} + \bar{u}}{R} + \beta\right) \cos KZ = \tau_{\theta\bar{\theta}} \cos KZ \tag{4}$$

$$\frac{\tau_{ZZ}}{2\mu_b \cos 2\theta} = (k\bar{w} + \beta) \cos KZ = \tau_{\bar{Z}Z} \cos KZ \tag{5}$$

$$\frac{\tau_{RZ}}{\mu_b \cos 2\theta} = \left(\frac{d\bar{w}}{dR} - K\bar{u}\right) \sin KZ = \tau_{\bar{R}Z} \sin KZ \tag{6}$$

$$\frac{\tau_{\theta Z}}{\mu_b \sin 2\theta} = -\left(K\bar{v} + 2\frac{\bar{w}}{R}\right) \sin KZ = \tau_{\theta\bar{Z}} \sin KZ \tag{7}$$

$$\frac{\tau_{R\theta}}{\mu_b \sin 2\theta} = \left(\frac{d\bar{v}}{dR} - \frac{2\bar{u} + \bar{v}}{R}\right) \cos KZ = \tau_{R\bar{\theta}} \cos KZ \tag{8}$$

where

$$\beta = \frac{\sigma}{1-2\sigma}\left(\frac{d\bar{u}}{dR}+\frac{2\bar{v}+\bar{u}}{R}+K\bar{w}\right).$$

Substitution of equations (3)–(8) into the equilibrium equations yields three differential equations involving $\bar{u}$, $\bar{v}$ and $\bar{w}$:

$$(1-\sigma)\frac{d^2\bar{u}}{dR^2}+\frac{(1-\sigma)}{R}\frac{d\bar{u}}{dR}+\frac{1}{R}\frac{d\bar{v}}{dR}+\frac{K}{2}\frac{d\bar{w}}{dR}-\left(\frac{3-5\sigma}{R^2}+\frac{1-2\sigma}{2}K^2\right)\bar{u}-\left(\frac{3-4\sigma}{R^2}\right)\bar{v}=0 \quad (9)$$

$$(1-2\sigma)\frac{d^2\bar{v}}{dR^2}+\frac{(1-2\sigma)}{R}\frac{d\bar{v}}{dR}-\frac{2}{R}\frac{d\bar{u}}{dR}-\left(\frac{9-10\sigma}{R^2}+K^2(1-2\sigma)\right)\bar{v}-\left(\frac{6-8\sigma}{R^2}\right)\bar{u}-\frac{2K}{R}\bar{w}=0 \quad (10)$$

$$(1-2\sigma)\frac{d^2\bar{w}}{dR^2}+\frac{(1-2\sigma)}{R}\frac{d\bar{w}}{dR}-k\frac{d\bar{u}}{dR}-\frac{k}{R}\bar{u}-\frac{2K}{R}\bar{v}-\left(\frac{4(1-2\sigma)}{R^2}+2K^2(1-\sigma)\right)\bar{w}=0. \quad (11)$$

The solution of equations (9)–(11) gives the radial distribution of $\bar{u}$, $\bar{v}$ and $\bar{w}$ and their derivatives, the actual stresses and displacements at any point being obtained by substitution into equations (2)–(8).

For each K value chosen equations (10)–(11) were solved numerically, using the Gill–Kutta procedure, to give three basic solutions to the elasticity equations. The first solution corresponded to loads of $\tau_{\bar{R}R} = 1{\cdot}0\tau_{\bar{R}\theta} = \tau_{\bar{R}Z} = 0$ on the loaded lateral boundary of the plate and zero values of these quantities on the unloaded boundary. The second and third solutions corresponded, in turn, to unit values of $\tau_{\bar{R}\theta}$ and $\tau_{\bar{R}Z}$, respectively on the loaded boundary, the remaining loads on both boundaries being zero.

For each plate thickness considered the overall stress distribution was obtained from a linear combination of the solutions corresponding to $K = 0$ with the outer lateral boundary of the plate loaded. From equation (2) it is seen that the axial displacement of this solution is zero and hence this is the "plane strain" solution. "Corrections" to this solution in the region of the hole were achieved by superimposing solutions corresponding to nineteen further values of K, with the inner lateral boundary loaded. The exact magnitude of the K values did not appear critical and an acceptable level of accuracy was achieved in each case by distributing the values of K. T between 0 and 10.

Great care, however, was needed in the positioning of points at which conditions were to be matched along the terminal boundary of the plate. In applications of the point matching technique it is essential to concentrate the points around the regions of high stress gradient since failure to do this will result in large errors in the boundary conditions between the matched points. This meant that a high concentration of points was required around the hole with a gradual reduction in intensity as the distance from the hole increased. However, the total number of points must be kept to a minimum to avoid unnecessary calculation. It was found in practice that between 50 and 60 matched points were sufficient for all the problems examined.

The regions away from the hole "plane" conditions exist and in order to simulate an infinite plate all solutions were truncated at $R = 20$ and the specified stresses at this boundary were those given by the "plane" solutions.

DISCUSSION OF RESULTS

Using the KT values and boundary points established previously, several thicknesses of plate were analysed for a material of Poisson's ratio of 0·25. This value of Poisson's

ratio was chosen so that a direct comparison could be made between the point matched results and those of Youngdahl and Sternberg [7] which were considered the most accurate of the previous solutions. Figures 1 and 2 show the axial variation of the hoop and axial stresses, respectively at $R = 1$ for various plate thicknesses. The boundary effect is clearly evident, its effect being more pronounced in thick plates. It is apparent that the "plane" solutions to this problem will only predict the axial and hoop stresses accurately in the region of the hole for two situations: (a) in the mid-section of thick plates where "plane strain" conditions exist and (b) in extremely thin plates where the boundary effect is negligible and "plane stress" conditions exist. However, the use of the "plane" solutions in establishing the stress concentration effect of the hole is justified as the maximum value of the hoop stress is predicted to within 4 per cent of its true value in the worst case.

Figure 3 indicates the axial variation of the displacements at $R = 1$. The radial, circumferential and axial displacements converge on their "plane stress" values for increasingly thin plates and for thick plates they approach their "plane strain" values at the mid-section. At the surface of thick plates the radial displacement approximates to its "plane stress" value. The hoop displacement increases from its "plane strain" value at the mid-section of the plate as if to attain its "plane stress" value at the surface. However, in a localized region near the surface of the plate, this displacement decays rapidly and is

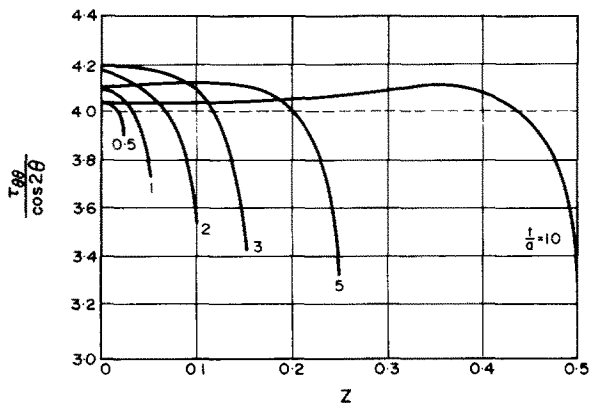

FIG. 1. Axial decay of hoop stress at $R = 1$.

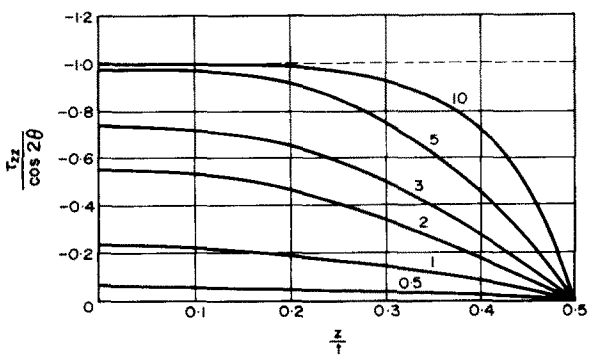

FIG. 2. Axial decay of axial stress at $R = 1$.

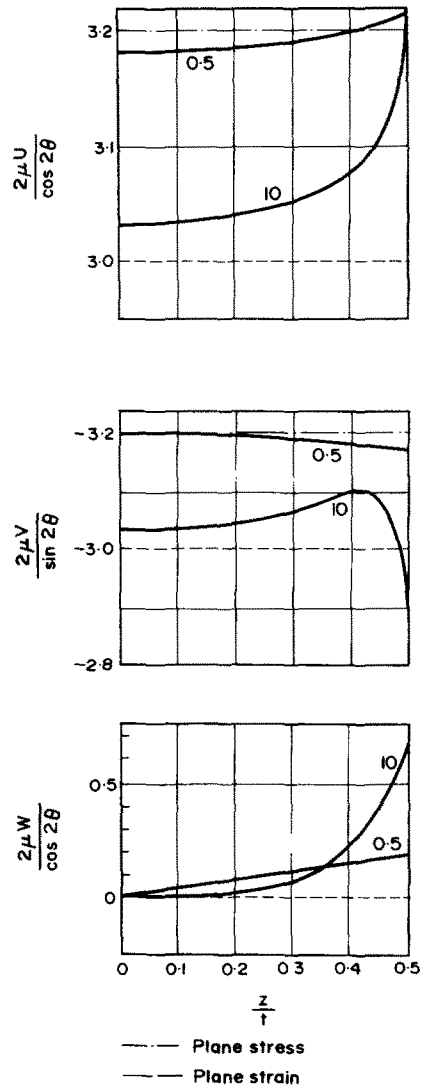

FIG. 3. Axial decay of U, V, W at $R = 1$.

considerably less than its "plane stress" value at the surface. The axial displacement is also affected by the boundary layer and its value at the surface is predicted reasonably accurately by the "plane stress" solution only when the thickness ratio of the plate is small.

To obtain the displacements transmitted to the base of the photoelastic gauge, the displacements experienced in stretching the plate prior to drilling the hole must be subtracted from the displacements determined above. These are:

$$2\mu_b U = R\cos 2\theta$$

$$2\mu_b V = -R\sin 2\theta$$

$$W = 0.$$

Thus the displacements appropriate to the gauge problem are obtained and the radial variation of these displacements at the metal surface is illustrated in Figs. 4 and 5 for a metal of Poisson's ratio 0·25. The radial and circumferential displacements approximate to their "plane stress" values, the circumferential displacement being approximately 10 per cent lower than this value. The axial displacements transmitted to the gauge are considerably greater than those predicted by the "plane" solutions, their values in a thick plate being in order of the Poisson's ratio times the radial displacement. For the purpose of obtaining the actual displacements to be used in the analysis of the photoelastic gauge, a metal of Poissons ratio 0·3 was chosen as representative of typical engineering materials. Thickness ratios $T = 10$ and $T = 0$ were used since these thicknesses produced the largest and smallest axial displacements. The displacements for $T = 10$ at the base of the gauge are illustrated in Fig. 6.

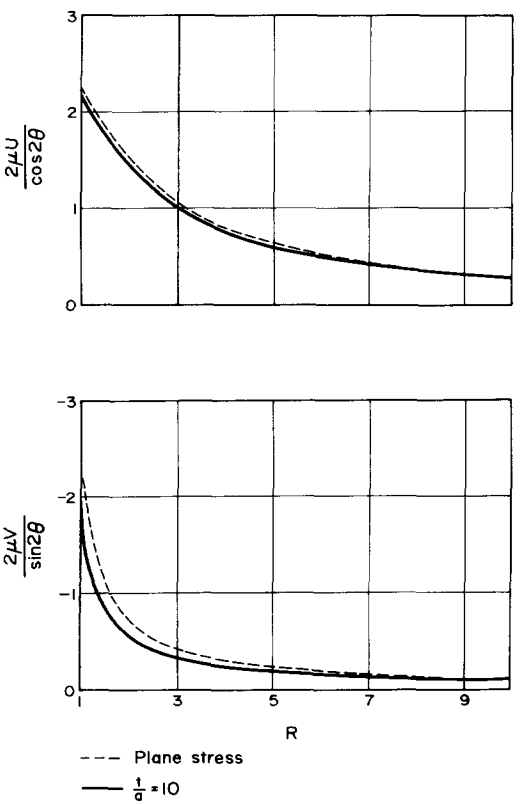

FIG. 4. Change in displacement at the surface of a metal of Poissons ratio of 0·25.

ACCURACY OF RESULTS

Comparison of the results obtained for a plate of thickness ratio $T = 10$ with those obtained by Youngdahl and Sternberg [7] for an infinitely thick plate show less than a 1 per cent discrepancy. The results obtained for thinner plates are assumed to have the

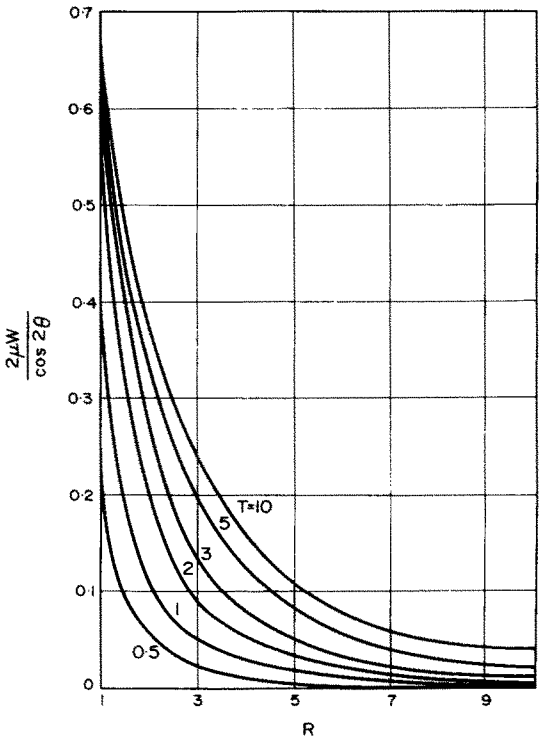

FIG. 5. Radial distribution of W at the surface of plates of various thickness ratios.

same accuracy since it was possible to match the boundary conditions even more accurately in these plates. The mean value of the errors in the matched conditions was less than 0·1 per cent for thin plates and less than 0·5 per cent in the plate of thickness ratio $T = 10$.

CONCLUSIONS

The stress concentration effect of holes in plates with equiaxial stresses of opposite sign is, for all practical purposes, independent of the thickness ratio of the plate. The maximum stress always occurs at the hole boundary and has a value slightly in excess of four. The displacements in the region of the hole, however, are not predicted with the same degree of accuracy by the "plane" solutions and thus the use of these in solving problems such as that of the "shear lag" problem would give erroneous results.

II. A THREE DIMENSIONAL ANALYSIS OF THE PHOTOELASTIC GAUGE

INTRODUCTION

THEORETICAL investigations into the "shear lag" effect in bonded photoelastic gauges in regions away from the gauge boundaries have been performed by Duffy [14] and Post and Zandman [15]. Investigations into this effect in the region of the hole in an annular

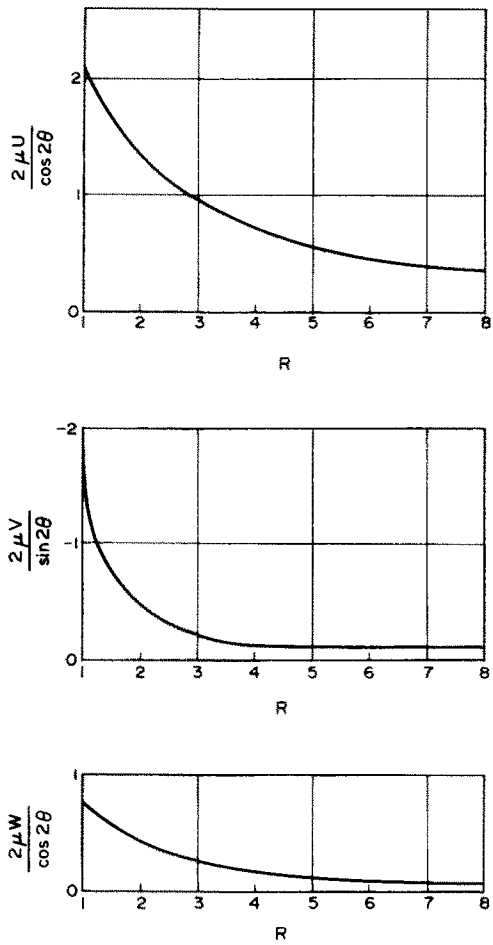

FIG. 6. Displacements transmitted to a gauge bonded to a metal of Poissons ratio = 0·3 and thickness ratio = 10.

gauge were initiated by Gibbs *et al.* [16] who used a relaxation technique to obtain an approximate solution for a gauge of a specific geometry. Subsequently Hooke and Stagg [17] obtained results for various gauge geometries by assuming zero axial displacement in the gauge and simulating the modified boundary conditions using a Fourier series loading.

Both of these latter theoretical solutions assumed a "plane strain" situation in the metal to obtain the displacements at the gauge–metal interface. From the results obtained in the previous section it is clear that this assumption is invalid.

Similarly the use of "plane" solutions in the analysis of the gauge is only justified for thin gauges in which the decay of the strains through the thickness is minimal. Even here the assumption of zero axial displacements in the gauge will only give accurate results when the axial displacements transmitted to the base of the gauge are small i.e. for a gauge bonded to a metal of a small thickness ratio.

Because of the limiting nature of the assumptions proposed above it was decided to obtain a complete three dimensional analysis of gauges of various geometries using a technique similar to the one used in determining the metal displacements.

CALCULATION OF THE STRESSES IN THE GAUGE

In Part I the stresses in the metal were assumed to be a combination of two basic stress systems. The displacements transmitted to the gauge by a metal loaded in the first system are given by the plane stress solution. They are:

$$U = \frac{1}{2\mu_b}\frac{1}{R}$$
$$V = W = 0. \tag{1}$$

The displacements at the gauge metal interface for the second system have been determined numerically in Part I and for a metal of Poisson's ratio 0·3 and thickness ratio $T = 10$ these are given in Fig. 6.

For a gauge attached to a metal loaded in either of these two systems the respective displacements form the boundary conditions along the base of the gauge. In both cases the conditions along the remaining boundaries of the gauge are:
at

$$R = 1$$

and

$$R = B \qquad \tau_{RR} = \tau_{RZ} = \tau_{R\theta} = 0$$

at

$$Z = T \qquad \tau_{ZZ} = \tau_{RZ} = \tau_{\theta Z} = 0. \tag{2}$$

In neither system do the "plane" solutions satisfy these boundary conditions and hence approximate three dimensional solutions for both systems have to be determined.

(a) *Equal principal stresses of the same sign*

The boundary conditions of this system suggest that an appropriate form of displacement function would be

$$2\mu_b U = \bar{u}\cos(KZ+\phi)$$
$$2\mu_b W = \bar{w}\sin(KZ+\phi) \tag{3}$$
$$V = 0$$

where the line $Z = 0$ corresponds to the base of the gauge, and $\bar{u}$ and $\bar{w}$ are functions of the radius only. No assumptions can be made as to the symmetry of the displacements in the gauge and an additional constant ϕ is introduced to allow for both symmetrical and skew symmetrical displacements.

Substituting equation (3) into the stress–displacement equations the following relationships are obtained:

$$\tau_{RR} = \frac{\mu_g}{\mu_b}\left(\frac{d\bar{u}}{dR} + \beta\right)\cos(KZ+\phi) = \frac{\mu_g}{\mu_b}\tau_{\bar{R}R}\cos(KZ+\phi) \tag{4}$$

$$\tau_{\theta\theta} = \frac{\mu_g}{\mu_b}\left(\frac{\bar{u}}{R} + \beta\right)\cos(KZ+\phi) = \frac{\mu_g}{\mu_b}\tau_{\bar{\theta}\theta}\cos(KZ+\phi) \tag{5}$$

$$\tau_{ZZ} = \frac{\mu_g}{\mu_b}(K\bar{w}+\beta)\cos(KZ+\phi) = \frac{\mu_g}{\mu_b}\tau_{Z\bar{Z}}\cos(KZ+\phi) \tag{6}$$

$$\tau_{RZ} = \frac{\mu_g}{2\mu_b}\left(\frac{d\bar{w}}{dR} - K\bar{u}\right)\sin(KZ+\phi) = \frac{\mu_g}{2\mu_b}\tau_{\bar{R}Z}\sin(KZ+\phi) \tag{7}$$

where

$$\beta = \frac{\sigma}{1-2\sigma}\left(\frac{d\bar{u}}{dR} + \frac{\bar{u}}{R} + K\bar{w}\right).$$

Substituting equations (4)–(7) into the equilibrium equations in the radial and axial directions the governing equations for $\bar{u}$ and $\bar{w}$, respectively, are obtained:

$$\frac{d^2\bar{u}}{dR^2} + \frac{1}{R}\frac{d\bar{u}}{dR} + \frac{K}{2-2\sigma}\frac{d\bar{w}}{dR} - \left(\frac{K^2}{2}\frac{1-2\sigma}{1-\sigma} + \frac{1}{R^2}\right)\bar{u} = 0 \tag{8}$$

$$\frac{d^2w}{dR^2} + \frac{1}{R}\frac{d\bar{w}}{dR} - \frac{K}{1-2\sigma}\left(\frac{d\bar{u}}{dR} + \frac{\bar{u}}{R}\right) - 2\,.\,K^2\frac{1-\sigma}{1-2\sigma}\bar{w} = 0. \tag{9}$$

Equations (8) and (9) were solved using the Gill–Kutta procedure. For each value of K chosen, eight basic solutions to the elasticity equations were obtained. Initially the plate was loaded with unit value of $\tau_{R\bar{R}}$ on the inner lateral boundary and, having solved for the radial distribution of the peak values of the displacements and their derivatives, two solutions were obtained by substituting these values into equations (3)–(7). The first solution was symmetrical with the constant ϕ equal to zero and the second solution was skew symmetrical with $\phi = \pi/2$. The next two solutions were obtained by repeating this procedure with a unit value of $\tau_{\bar{R}Z}$ on the inner lateral boundary. The remaining four solutions were obtained by repeating the procedure for the previous four except that the loads were transferred to the outer lateral boundary, the inner lateral boundary being unloaded. It was considered necessary to use solutions that decayed from both the lateral boundaries of the gauge because of the unpredictable nature of the shear lag effect in these regions.

For each gauge thickness considered a number of these basic solutions for a range of values of K were superimposed so as to satisfy the boundary conditions in a least squares manner.

At any given point in the gauge the difference between the radial and hoop stresses was then given by

$$(\tau_{RR} - \tau_{\theta\theta}) = \frac{\mu_g}{\mu_b}\sum_{n=1}^{q} a_n(\tau_{R\bar{R}} - \tau_{\bar{\theta}\theta})_n \cos K_m Z \tag{10}$$

where K_m is the constant associated with the nth solution and q is the total number of basic solutions used.

The photoelastic effect observed depends upon the product of the thickness of the gauge and the mean value of the principal stress difference:

$$(\tau_{RR}-\tau_{\theta\theta})_{\text{mean}} = \frac{1}{T}\int_0^T (\tau_{RR}-\tau_{\theta\theta})\,\mathrm{d}Z \tag{11}$$

which upon integration gives

$$(\tau_{RR}-\tau_{\theta\theta})_{\text{mean}} = \frac{\mu_g}{\mu_b} A\left(\frac{r}{a}\right)$$

where

$$A\left(\frac{r}{a}\right) = \frac{1}{T}\sum_{n=1}^{q} \frac{\alpha_n(\tau_{\bar{R}R}-\tau_{\theta\bar{\theta}})_n(\sin K_m T-\sin\phi)}{K_m}$$

The actual fringe order (N) observed for a photoelastic material of fringe coefficient f and thickness t is then given by:

$$N = \frac{2t}{f}\frac{\mu_g}{\mu_b} A\left(\frac{r}{a}\right). \tag{12}$$

(b) *Equal principal stresses of opposite sign*

The displacement functions appropriate to the second stress system are:

$$\begin{aligned} 2\mu_b U &= \bar{u}\cos(KZ+\phi)\cos 2\theta \\ 2\mu_b V &= \bar{v}\cos(KZ+\phi)\sin 2\theta \\ 2\mu_b W &= \bar{w}\sin(KZ+\phi)\cos 2\theta. \end{aligned} \tag{13}$$

These are identical to those used in Part I except for the introduction of the constants μ_b and ϕ. The stresses are therefore given by equations (3)–(8) of Part I with the constant ϕ introduced in the sinusoidal terms and the stresses multiplied by the factor $\mu_g/2\mu_b^2$. None of these modifications affect the governing equations for $\bar{u}$, $\bar{v}$ and $\bar{w}$ which are given by equations (9), (10) and (11) of Part I, respectively.

For each K value chosen, 12 basic solutions to elasticity equations were obtained. These solutions corresponded to the loadings used for a gauge loaded in the first system except that an additional four solutions were obtained corresponding to unit values of $\tau_{R\bar{\theta}}$ on the inner and outer lateral boundaries of the gauge for each of the values of ϕ of 0 and $\pi/2$. As before the mean values of the required stresses at any radius were obtained.

$$\frac{(\tau_{RR}-\tau_{\theta\theta})_{\text{mean}}}{\cos 2\theta} = \frac{1}{T}\frac{\mu_g}{\mu_b}\sum_{n=1}^{q} \frac{a_n(\tau_{\bar{R}R}-\tau_{\bar{\theta}\theta})_n(\sin K_m T-\sin\phi)}{K_m} = \frac{\mu_g}{\mu_b} B\left(\frac{r}{a}\right) \tag{14}$$

$$\frac{(2\tau_{r\theta})_{\text{mean}}}{\sin 2\theta} = \frac{1}{T}\frac{\mu_g}{\mu_b}\sum_{n=1}^{q} \frac{a_n(\tau_{\bar{R}\theta})_n(\sin K_m T-\sin\theta)}{K_m} = \frac{\mu_g}{\mu_b} C\left(\frac{r}{a}\right) \tag{15}$$

The difference between the principal stresses at any radius is then given by

$$\{(\tau_{RR}-\tau_{\theta\theta})^2_{\text{mean}}+(2\tau_{r\theta})^2_{\text{mean}}\}^{\frac{1}{2}} \tag{16}$$

and hence the fringe order is

$$N=\frac{2t}{f}\frac{\mu_g}{\mu_b}\left\{B^2\left(\frac{r}{a}\right)\cos^2 2\theta+C^2\left(\frac{r}{a}\right)\sin^2 2\theta\right\}^{\frac{1}{2}}. \tag{17}$$

INTERPRETATION OF FRINGE PATTERNS

When the principal stresses are neither equal nor opposite the fringe orders may be obtained by taking appropriate combinations of equations (12) and (17). For principal stresses given by S_1 and S_2 the fringe order at radius r and angle θ to the stress S_1 will be

$$N=\frac{2t}{f}\frac{\mu_g}{\mu_b}\left\{\left(\frac{S_1+S_2}{2}A\left(\frac{r}{a}\right)+\frac{S_1-S_2}{2}B\left(\frac{r}{a}\right)\cos 2\theta\right)^2+\left(\frac{S_1-S_2}{2}C\left(\frac{r}{a}\right)\sin 2\theta\right)^2\right\}^{\frac{1}{2}}. \tag{18}$$

It follows that the directions of the principal stresses coincide with the axes of symmetry of the fringe pattern. Furthermore the fringe orders at $\theta = 0$ and $\theta = 90°$, respectively, are given by

$$N_1=\frac{2t}{f}\frac{\mu_g}{\mu_b}\left\{\frac{S_1+S_2}{2}A\left(\frac{r}{a}\right)+\frac{(S_1-S_2)}{2}B\left(\frac{r}{a}\right)\right\} \tag{19}$$

$$N_2=\frac{2t}{f}\frac{\mu_g}{\mu_b}\left\{\frac{S_1+S_2}{2}A\left(\frac{r}{a}\right)-\frac{(S_1-S_2)}{2}B\left(\frac{r}{a}\right)\right\}. \tag{20}$$

By rearranging equations (19) and (20) the principal stresses may be found in terms of N_1 and N_2:

$$S_1=\frac{f}{2t}\frac{\mu_b}{\mu_g}\left\{\frac{N_1}{2}\cdot\frac{A\left(\frac{r}{a}\right)+B\left(\frac{r}{a}\right)}{A\left(\frac{r}{a}\right)B\left(\frac{r}{a}\right)}+\frac{N_2}{2}\frac{B\left(\frac{r}{a}\right)-A\left(\frac{r}{a}\right)}{A\left(\frac{r}{a}\right)B\left(\frac{r}{a}\right)}\right\} \tag{21}$$

$$S_2=\frac{f}{2t}\frac{\mu_b}{\mu_g}\left\{\frac{N_2}{2}\frac{A\left(\frac{r}{a}\right)+B\left(\frac{r}{a}\right)}{A\left(\frac{r}{a}\right)B\left(\frac{r}{a}\right)}+\frac{N_1}{2}\frac{B\left(\frac{r}{a}\right)-A\left(\frac{r}{a}\right)}{A\left(\frac{r}{a}\right)B\left(\frac{r}{a}\right)}\right\}. \tag{22}$$

APPLICATION OF THE POINT MATCHING TECHNIQUE TO GAUGES OF VARIOUS THICKNESSES

The application of the point matching technique to the gauge problem poses several difficulties not encountered in the determination of the metal displacements.

The boundary conditions of the gauge are mixed i.e. displacements are specified over part of the boundary and stresses over the remainder of the boundary. It was found that the stresses were accurately matched but the displacements being far smaller numerically were poorly matched. This difficulty was overcome by matching displacements multiplied by the factor $2\mu_g/R$ which made them comparable in magnitude to the stresses.

Great difficulty was also experienced in matching the boundary conditions at the junctions of the inner and outer lateral boundaries of the gauge and the metal. At these junctions the displacements must be compatible with those specified along the gauge metal interface and at the same time give zero radial and shear stresses to satisfy the conditions on the lateral boundaries of the gauge. This gives a discontinuity in the radial stress and infinite shear stress gradients at these junctions and these were impossible to match using the continuous form of solution established previously. It was considered that a small surface stress would have minimal effect on the stress distribution in the gauge and only the displacement conditions were matched at these points.

The choice of K values was also given more consideration than had previously seemed necessary. The number of solutions associated with each K value in the gauge problem was far greater than in the plate problem and thus it was essential to choose the values of K carefully so as to avoid forming an unnecessary large number of basic solutions. In practice it was found that conditions could be accurately matched using less than half the number of K values used previously.

For thin gauges loaded in the first system the "plane strain" solution closely approximated the actual stress distribution in the gauge and "corrections" in the region of the hole were readily achieved by using solutions corresponding to a few high K values. For thicker gauges two K values were used to provide the localized "corrections" near the hole and an even distribution of lower K values was used to match the shear lag effect in regions away from the hole. Consequently the majority of the results were obtained using solutions corresponding to KT values of 0·5, 1, 2, 3, 4, 5, 7·5 and 9.

For thin gauges loaded in the second stress system solutions corresponding to several low K values together with the solutions corresponding to $K = 0$ were used to give the overall stress distribution. The selection of the K values of the remaining solutions was similar to that explained above and results were obtained using KT values of 0, 0·1, 0·4, 1, 2, 3, 4, 6, 9. The positioning of boundary points was similar to that used in the plate problem. However, in this problem the solutions decayed from both the inner and outer lateral boundaries of the gauge and it was necessary to use a dense point population in both these regions.

DISCUSSION OF RESULTS

(a) *Equal principal stresses*

Figure 7 indicates the variation of $(\tau_{RR} - \tau_{\theta\theta})$ through the thickness of various gauges at $R = 2$, the "shear lag" effect being especially pronounced in thicker gauges. Figure 8 shows the radial variation of $A(r/a)$ for a gauge material of Poisson's ratio 0·36 and outer

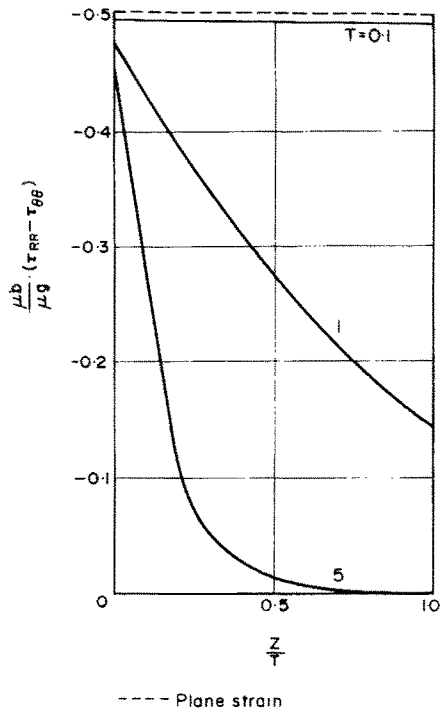

FIG. 7. "Shear lag" effect in gauges loaded in the first stress system.

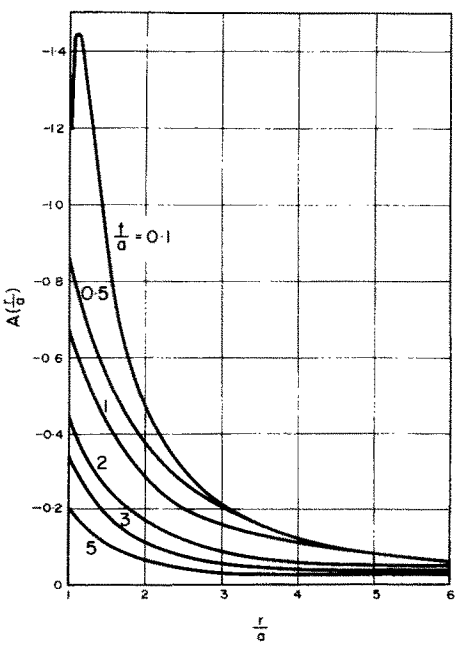

FIG. 8. Variation of $A(r/a)$ with radius.

radius $b/a = 8$. The curve for $t/a = 0{\cdot}1$ follows extremely closely the plane solutions except in the immediate vicinity of the hole where the rapid decay of the radial stress produces a lower fringe order than that predicted by the latter solution. For thicker gauges the prediction of fringe orders by the "plane" solutions becomes increasingly erroneous both in the region of the hole and away from this region.

(b) *Equal and opposite principal stresses*

In this system the axial displacements transmitted to the gauge are significantly dependent upon the thickness ratio of the metal. In order to establish the significance of these displacements two cases were considered which were (a) a metal of extremely small thickness ratio in which the axial displacements are given by the "plane stress" solutions, (b) a metal of thickness ratio $T = 10$ in which the axial displacements have reached their maximum value. The Poisson's ratios of the metal and gauge material were 0·30 and 0·36, respectively, and the outer diameter of the gauge was at $R = 8$.

Figures 9 and 10 indicate the radial distribution of $B(r/a)$ and $C(r/a)$ for case (a), the corresponding curves for case (b) being given in Figs. 11 and 12. The values of the coefficients B and C are significantly increased in case (b) the difference being more pronounced in these gauges. The prime reason for this increase is seen by considering the curves for a gauge of thickness ratio $T = 0$ in Fig. 13. This figure indicates the "shear lag"

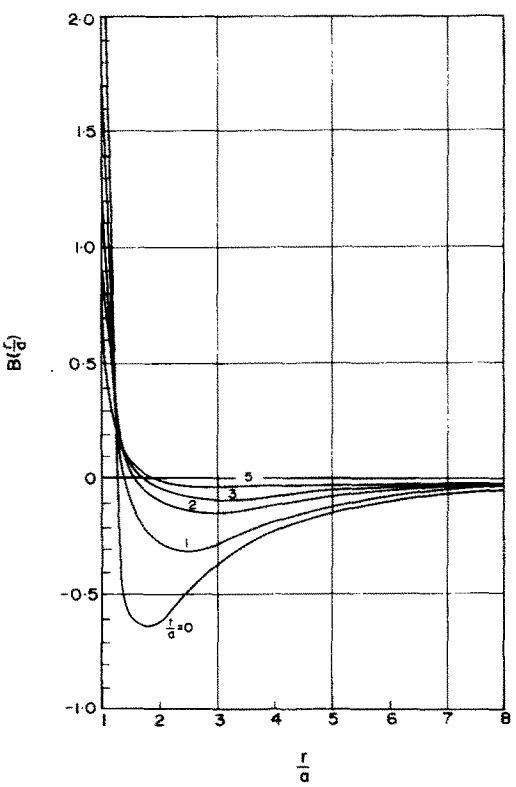

FIG. 9. $B(r/a)$ for gauges bonded to a metal of Poissons ratio = 0·3 and thickness ratio = 0.

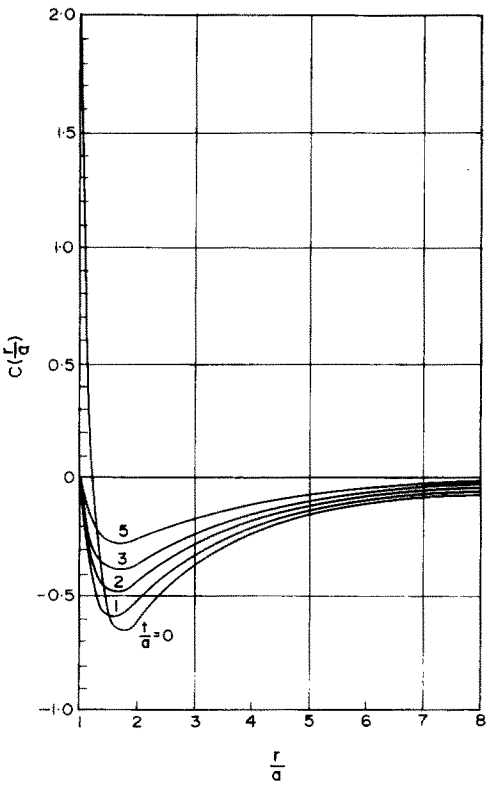

FIG. 10. $C(r/a)$ for gauges bonded to a metal of Poissons ratio = 0·3 and thickness ratio = 0.

effect of gauges loaded in the second stress system, the "thin plate" curves corresponding to case (a) and the "thick plate" to case (b). The curves for $T = 0$ were obtained by multiplying the appropriate stress values at the surface of the metal by the ratio of the shear modulus of the metal to that of the gauge. In case (b) the "boundary layer" effect in the metal was pronounced and consequently the values of $(\tau_{RR} - \tau_{\theta\theta})$ and $\tau_{R\theta}$ at the base of the gauge were greater than those predicted by the "plane stress" solution used in case (a). For infinitely thin gauges, in which the "shear lag" effect is negligible, the coefficients $B(r/a)$ and $C(r/a)$ were correspondingly increased.

These coefficients were further increased by the bending effect of the axial displacements in case (b) as indicated by the curves for $T = 0{\cdot}1$. For this gauge thickness the stress quantities increase linearly through the thickness of the gauge, an effect which is in direct contradiction to the "shear lag" effect. The bending effect is confined to a localized region near the base of the gauge and is of negligible importance in thicker gauges where the stresses decay through the thickness of the gauge in the usual manner. In the thicker gauges a boundary layer effect is again experienced near the surface of the gauge, this effect being most noticeable in a gauge of thickness ratio $T = 1$. In thicker gauges the shear lag effect is predominant in producing coefficients in cases (a) and (b) which are in close agreement.

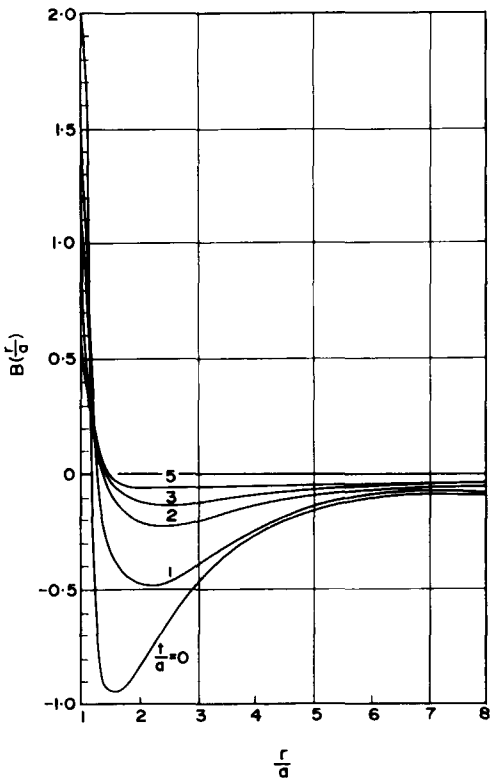

FIG. 11. $B(r/a)$ for gauges bonded to a metal of Poissons ratio = 0·3 and thickness ratio = 10.

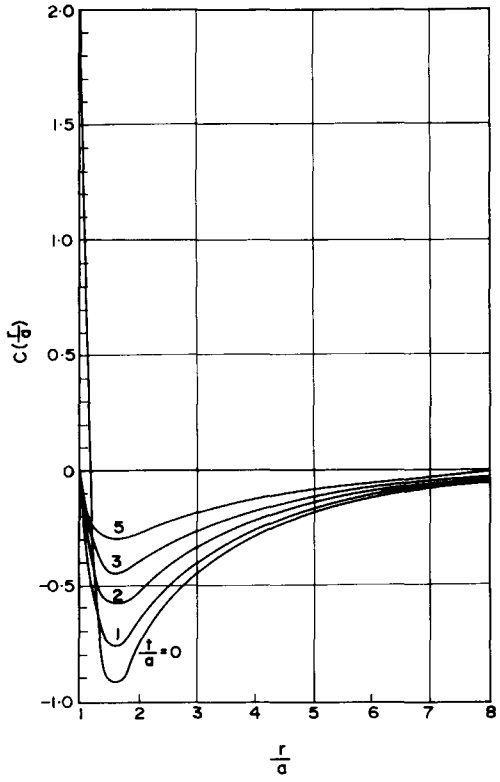

FIG. 12. $C(r/a)$ for gauges bonded to a metal of Poissons ratio = 0·3 and thickness ratio = 10.

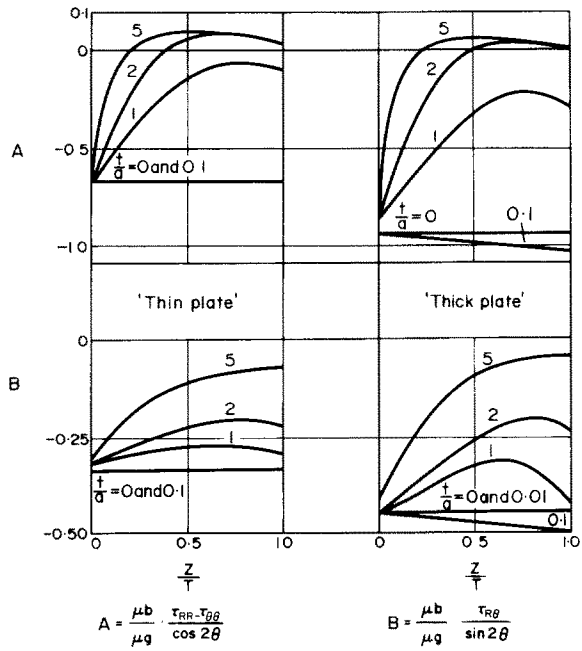

FIG. 13. "Shear lag" effect in gauges loaded in second stress system.

RECOMMENDED HOLE AND GAUGE DIMENSION FOR THE PRACTICAL APPLICATION OF THE TECHNIQUE

The theory presented in this paper assumes that the diameter of the hole is small when compared to the outer dimensions of the metal and consequently this criterion must be observed in any practical application of the technique. Fringe coefficients have been determined for two ratios of plate thickness to hole radius, i.e. $T = 0$ and $T = 10$. It was shown that the coefficients $B(r/a)$ and $C(r/a)$ are significantly dependent upon this latter ratio and for any thickness ratio other than the two aforementioned values it is necessary to interpolate between the two sets of results to obtain the appropriate fringe coefficients for the chosen thickness ratio. To avoid this interpolation it is suggested that the hole diameter should either be (a) large when compared to the thickness of the plate but small when compared to its outer dimensions in which case the fringe coefficients in case (a) can be used; or (b) the hole diameter should be less than half of the depth of the residual stresses in which case the coefficients obtained in case (b) apply.

The results obtained in this paper are for a ratio of the outer radius of the gauge to the hole radius of 8. Increasing this value has little effect on the stress distribution. This value should therefore be regarded as the minimum ratio for which the results presented here apply.

In normal applications of the photoelastic technique it is advantageous to use a large material thickness to obtain high fringe orders. However, in this particular application this increase is effectively nullified by the increased shear lag effect and there is no advantage in using gauges of greater thickness than the hole diameter.

CONCLUSIONS

The effect of "shear lag" in annular photoelastic gauges has been successfully analysed. Accurate fringe coefficients have been determined for the use of the gauges in the "hole drilling" technique. The use of these coefficients eliminates any errors due to "shear lag" which, if neglected, would in practice lead to an underestimation of the residual stresses of about 50 per cent even with relatively thin gauges. Recommendations have been made as to suitable dimensions for the hole and gauge.

REFERENCES

[1] M. NISIDA, A Method of Stress Measurement, Br. Pat. Spec. 938, 289 (1963).
[2] M. NISIDA and H. TAKABAYASHI, Thickness Effects in "Hole Method" and Applications of the Method to Residual Stress Measurement, *Proc. 13th Natn. Congr. Appl. Mech.* (1963).
[3] E. RESSNER, On the Calculation of Three Dimensional Corrections to the Two Dimensional Theory of Plane Stress, *Proc. 15 Semi Annual Eastern Photoelasticity Conference* (1942).
[4] A. E. GREEN, The elastic equilibrium of isotropic plates and cylinders. *Proc. R. Soc.* **A195**, 153 (1949).
[5] E. STERNBERG and M. A. SADOWSKY, Three dimensional solution for the stress concentration around a circular hole in a plate of arbitrary thickness. *J. appl. Mech.* **16**, 27 (1949).
[6] E. L. REISS and S. LOCKE, On the theory of plane stress. *Q. Jl appl. Math.* **19**, 165 (1961).
[7] C. K. YOUNGDAHL and E. STERNBERG, Three dimensional stress concentration around a circular hole in a semi-infinite elastic plate. *J. appl. Mech.* **33**, 865 (1966).
[8] I. U. OJALVO and F. D. LUIZER, Improved point matching techniques. *Q. Jl applied Math. Mech.* **18**, 41 (1945).
[9] H. D. CONWAY and A. W. LEISSA, The application of the point matching technique to shallow-spherical shell theory. *J. appl. Mech.* 745 (1962).
[10] F. W. NIEDENFUHR and A. W. LEISSA, Bending of a square plate with two adjacent edges free and others clamped or simply supported. *AIAA Jnl* **1**, 116 (1963).
[11] L. E. HUBERT and F. W. NIEDENFUHR, Accurate calculation of the stress distribution in multiholed plates. *J. Engng Ind.* (1965); *Trans. Am. Soc. mech. Engrs* **B87**, 331.
[12] C. J. HOOKE, Numerical solution of plane elastostatic problems by point matching. *J. Strain Anal.* **3**, 109 (1968).
[13] C. J. HOOKE, Numerical solution of axisymmetric problems. *J. Strain Anal.* 25 (1970).
[14] J. DUFFY, Effect of thickness of birefringent coatings. *Proc. Soc. exp. Stress Analysis* **18**, 74 (1961).
[15] D. POST and F. ZANDMAN, Accuracy of birefringent method for coatings of arbitrary thickness. *Proc. Soc. exp. Stress Analysis* **18**, 21 (1961).
[16] H. G. GIBBS, C. J. HOOKE and J. J. STAGG, An Application of Photoelastic Changes to the measurement of Residual Stresses VDI Ber No. 102 (1966).
[17] C. J. HOOKE and J. J. STAGG, An approximate solution for the effect of "shear lag" in the measurement of residual stresses using a photoelastic gauge. *Int. J. Solids Struct.* **4**, 139 (1968).

APPENDIX

The application of the point matching technique to any boundary value problem in elasticity involves initially determining a number of basic solutions to the elasticity equations. The prescribed boundary conditions at a number of points on the boundary of a body are then satisfied by superpositioning a number of these solutions.

Suppose at a typical point i on the boundary the prescribed normal stress or displacement is N_i and the two prescribed tangential stresses or displacements are T_i and V_i. These normal and tangential quantities are then calculated for each of the basic solutions at each point on the boundary. The criterion then used in satisfying the boundary conditions is that the sum of the squares of the errors in the boundary conditions at the N points shall be a minimum.

The sum of the squares of the errors is given by

$$\sum_{i=1}^{N} (E_i)^2 = \sum_{i=1}^{N} \left(N_i - \sum_{k=1}^{q} a_k N_{ki} \right)^2 + \left(T_i - \sum_{k=1}^{q} a_k T_{ki} \right)^2 + \left(V_i - \sum_{k=1}^{q} a_k V_{ki} \right)^2$$

where N_{ki}, T_{ki} and V_{ki} are the normal and tangential quantities, at the point i, as given by the kth solution and a_k is the unknown coefficient associated with this solution. Differentiating the above expression with respect to each of the unknowns in turn a set of q simultaneous equations for the q unknown constants is obtained.

$$\sum_{i=1}^{N} (N_i N_{mi} + T_i T_{mi} + V_i V_{mi}) = \sum_{k=1}^{q} \sum_{i=1}^{N} a_k (N_{ki} N_{mi} + T_{ki} T_{mi} + V_{ki} V_{mi}) \qquad m = 1, 2, 3 \ldots q.$$

These equations are then solved for the unknown constants and the final solution is obtained by superposition of the basic solutions in their appropriate proportions.

(*Received* 5 *April* 1971)

Абстракт—Одним из методов измерения остаточных напряжений в металлах является присоединение кольцегого фотоупругого диска к поверхности металла и сверление центрического отверстия, сквозь датчик, в ниже находящиися материале. Если смотреть на датчик в полеризационнм свете, наблюдается образ интерференционных полос. Цель настоящей работы состоит в получений несложной „надлежащей" зависимости между порядками интеференционных полос из измерений и остаточными существующими напряжениями. Частв I обсуждает вопрос расчета перемещений в метталах. В части II, определяется положение суммарных напряжений в датчике. Затем представляются факторы градуировкм для широкого круга геометрии датчиков.